Identification of suspension state using Passive Acoustic Emission and Machine Learning in a solid-liquid mixing system.

Alberto Rossi[1,2], Federico Alberini[2*], Elisabetta Brunazzi[1]
[1] *Department of Civil and Industrial Engineering, University of Pisa, I-56126, Pisa, Italy*
[2] *School of Chemical Engineering, University of Birmingham, Edgbaston, B15 2TT, UK*

**Corresponding author: f.alberini@bham.ac.uk*

Abstract

Solid-Liquid mixing is a core operation in many manufacturing processes in the food, cosmetics, pharmaceutical and chemical industries.
This work aims to develop an accurate and reliable sensing methodology using Passive Acoustic Emission (PAE) coupled with Supervised Machine Learning (ML) algorithms, to allow identifying and predicting Solid-Liquid suspension state.
Using PAE in process monitoring is beneficial because it is are affordable, sensitive, non-intrusive, and suitable for on-line applications. PAE equipment includes a piezoelectric sensor, placed in contact with the system, an amplifier, a filter, an oscilloscope to record the signal and a computer.
Experiments were carried out in a fully baffled, flat bottom glass vessel equipped with a PBT impeller. Acoustic signals were recorded with sampling frequency of 750 kHz, impeller speed range 50-1,000 rpm and varying solid features, i.e., particle size (dp range 0.250-6 mm), solid loading and solid density (acryl-glass particles).
For each classification run, sampled data were pre-processed using Fast Fourier Transform (FFT) to reveal any detailed spectral characteristics of the signal in the frequency domain. Spectra have been filtered and then reduced by selecting the highest variance frequencies. As labelling, established optical measurements were used to classify the acoustic frequency spectra.
The frequency data set has been split in Training (60%), Cross validation (20%) and Test (20%) sets and were used, respectively, to build the model, identify the best model parameters (Optimisation step), and finally to check the accuracy (Test Step).
The developed technique has shown excellent results in recognizing spectra corresponding to different classes with observed accuracy greater than 99.72%.

Abbreviations and Symbols

AE	Acoustic Emission
B	Baffle width
C	Impeller off-bottom Clearance
CH	Cloud Heigh
CLA	Classification Learner Application
D	Impeller Diameter
Dp	Particle Diameter
DFT	Discrete Fourier Transform
FFT	Fast Fourier Transform
JS	Just Suspended
k-NN	k-Nearest Neighbour
N_{JS}	Just Suspended impeller speed
N_U	Uniform Suspension impeller speed
ML	Machine Learning
PAE	Passive Acoustic Emission
PBT	Pitched Blade Turbine
PC	Principal Components
PCA	Principal Components Analysis
RV	Relative Variance
S-L	Solid - Liquid
SVM	Support Vector Machine
T	Tank Diameter
TREE	Fine tree algorithm
Z	Liquid Height

1 Introduction

In recent years, the *Smart Manufacturing* perspective has significantly impacted the management processes in industrial field, supporting the build-up of smart environment and networks that are representative of the changes in the industrial model (Davis *et al.*, 2012; Lele, 2019).
In these challenges, new, dynamic, and flexible technologies, capable of extracting data in real time from the physical production system, are continuously required (Lee, Bagheri and Kao, 2015). Therefore, the current monitoring tools are always evolving and need to be improved. In addition, a further challenge is presented in managing and analysing the collected data efficiently.

Solid-Liquid (S-L) mixing plays a significant role in industrial operations, such as adsorption, crystallisation, leaching, reaction on solid-catalyst (Paul, Atiemo-Obeng and Kresta, 2004)(Nienow, Edward and Harnby, 1997).
These processes are mostly performed in stirred tank units, specially designed to ensure high contact area between the phases and avoid solid build-up at the bottom of the tank. Supplying power to the impeller promotes the motion of the fluid, and consequently, the momentum transfer, thus enhancing the solid particle motion within the continuous phase (liquid).
Three main suspension states (commonly referred to as *Partial, Complete, Uniform*)(Nienow, 1985; Paul, Atiemo-Obeng and Kresta, 2004) are used in the literature to describe the mixing quality of the blending of solids in liquid.
Over the years, huge efforts have been devoted by the research community to link the complex hydrodynamics (Cleaver and Yates, 1973; Baldi, Conti and Alaria, 1978; Buurman, Resoort and Plaschkes, 1986; Barresi and Baldi, 1987) and the suspension state. The complexity in terms of suspension level, energy demand, transfer phenomena (Kneule, 1956; Harriott, 1962a; Nienow, Unahabhokha and Mullin, 1969; Nagata, 1975) and quantity of affecting variables, such as physical properties of liquid and solid, operating conditions, geometrical parameters and agitation conditions, make this subject very challenging with still many unanswered questions.
Understanding the solid-liquid interactions has been one of the most discussed topics since the 1950's. In this perspective, papers have been published with regularity, a wide number of experiments have been carried out, and several empirical models have been presented where Zwietering correlation is the starting point (Zwietering, 1958; Harriott, 1962b; Nienow, 1968; Nienow, Unahabhokha and Mullin, 1969; Nagata, 1975; Guerci, Conti and Sicardi, 1986; Raghava Rao, Rewatkar and Joshi, 1988). As a consequence of the Zwietering correlation's "just suspended" definition (Zwietering, 1958), the results of all efforts inevitably lead to a certain degree of discrepancies and confusion.

A wide number of experimental techniques have been developed to identify the critical agitation (i.e., the Just Suspended condition, JS) or to quantify solid suspension in terms of solid concentration profile (Brunazzi *et al.*, 2002, 2004). But generally, their applicability suffers laboratory condition limits ('M. Bohnet, G. Niesmak, Distribution of solids in stirred suspensions, Germ. Chem. Eng. 3 (1980) 57–65.', no date; Bourne and Sharma, 1974; Barresi

and Baldi, 1987; D. Havelkova, 1987; Raghava Rao, Rewatkar and Joshi, 1988; Ayazi Shamlou and Koutsakos, 1989; Micale, Grisafi and Brucato, 2002; Špidla *et al.*, 2005; Angst and Kraume, 2006; Jirout, Moravec and Rieger, 2006; Shirhatti *et al.*, 2007; Hosseini *et al.*, 2010; Jafari, Tanguy and Chaouki, 2012; Tervasmäki, Tiihonen and Ojamo, 2014). Most of them were proven to have limited industrial applicability and inadequate to be integrated with real-time detection methods (Forte *et al.*, 2019).
In order to achieve on-time process knowledge and, hence, to control the quality, new methods are required.
This work focuses on the development of a smart and reliable technique to monitor the mixing process, more precisely identifying and predicting solid-liquid suspension state by making use of acoustic emission and machine learning. The objective is to potentially overcome the typical drawbacks of common experimental methodologies such as intrusiveness, affordability and need for non-opaque vessels.

PAE (Boyd and Varley, 2001), requires an acoustic sensor to be placed in contact with the outer wall of the vessel, which ensures non-invasive interaction with the mixing system, no safety issues, and applicability on opaque vessels and mixtures (Forte *et al.*, 2021).
Moreover, it allows to simply "listen" to the flow features making use of compact and affordable equipment and collecting data in real time (Grosse and Ohtsu, 2008).
There have been several positive attempts with AE which demonstrated that statistical and spectral features of the signals are sensitive to variation in (S-L mixing) physical characteristics e.g. particle diameter, solid loading and density (Belchamber *et al.*, 1986; Tily *et al.*, 1988; Bouchard, Payne and Szyszko, 1994; Hou, Hunt and Williams, 1999). However, the AE from solid suspension in stirred vessels has been explored only in recent years (He, Wang and Yang, 2009; Sardeshpande *et al.*, 2009).

The massive data input from AE is a positive but also challenging aspect of this technology. This is why Machine Learning (ML) techniques (L'Heureux *et al.*, 2017) have been employed to help and tackle the problem of understanding the data. ML tools aim to detect hidden patterns in the analysed data from the same rules that can be used to formulate decisions and predictions, hence, to solve classification or regression problems in case the model will provide discrete or continuous responses respectively (Mitchell, 1997; Simon *et al.*, 2015; Kubat, 2017).
Supervised ML algorithms which are widely used in Manufacturing fields (Wuest *et al.*, 2016) have been used in this study. This involves learning from an initial training step (on labelled examples) that allows to build a prediction model. Once the model is optimised, it can be tested on new unseen data to provide the belonging category as the prediction output (classification problem) by quickly processing the acoustic signal.

Thus, the goal was to investigate the solid-liquid suspension state by means of its effects on AE fingerprint. This led towards the development of a relatively simple and affordable methodology to discern the classes and provide information on what was occurring in the mixer without directly looking inside, which is highly desirable in both academic studies and industrial applications.

2 Materials & Methods

2.1 The S-L system

The experiments were conducted in a flat-bottomed stirred tank from Electrolab (Electrolab Biotech Ltd, UK) with inner diameter T = 160 mm and four equally spaced baffles (B=T/10). The agitation was provided by a six-bladed pitched turbine (PBT6) in down-pumping configuration with diameter D = 64 mm (D/T = 2/5) and positioned with an off-bottom clearance C=T/4.
The 6 L glass vessel was filled with water up to a height Z = T, so that the working volume was 3.25 L.
Monodispersed acrylic (density = 1031 kg/m^3) and glass (density = 2450 kg/m^3) spherical particles with different diameters were selected: i.e., 2.5, 4, 6 mm for acrylic and 0.250, 0.650, 1.250 mm for glass particle, respectively, at a volume concentration of X_{vol} = 0.435%, where X = volume of solid/(volume of solid+liquid).
The X_{vol} was selected to facilitate reliable and meaningful results for the two optical techniques used for the validation. In fact, the overall aim of this work is to validate this technique based on passive AE, independently from the system of reference. Measurements were taken at 20 different impeller rotational speeds in the range N = 50-1,000 rpm, with an interval of 50 rpm between each speed.
Moreover, the selection of materials and sizes for the particles, was driven by the desire of validating this new methodology for the monitoring of solid-liquid mixing in different physical environments. This is particularly relevant to tackle the often criticized versatility of machine learning techniques in slightly different applied environments.

2.2 Suspension States identification

The suspension state identification represents a preliminary step that is required to provide labels for the acoustic data for the necessary training of ML algorithms.
The acrylic systems were studied by means of the traditional visual technique as their low solid concentration makes this technique suitable to be uniquely adopted.
The *Visual identification* approach was based on the examination of 2 sec video sequences of side and bottom views of the system recorded by means of a high-speed camera FASTCAM SA3 (PHOTRON, Japan) at 250 fps and 12-bit dynamic range.
The video analysis was carried out on PFV3 software (PHOTRON FASTCAM Viewer3, Japan) that allows reading, handling, and saving the video files.
The Njs condition was observed according to the Zwietering criterion (Zwietering, 1958) by means of both bottom and side views; while the side views were used to focus the *Uniform suspension,* defined as the mixing condition whereby the cloud of solid particles reaches the liquid surface.

While for acrylic systems the transition from settled to suspension states occurred in a narrow range of N, with the heavier glass particles, a more progressive transition was observed. Therefore, particular care was paid to identifying the JS mixing condition for the glass systems.

For this reason, the visual approach was supported by a quantitative technique (*Image processing*) to enable the objectivity and cross-validation of the measurements.

The herein adopted *Image processing technique* (Ye, Nienow and Alberini, 2019), recently proposed as a quantitative method to identify Njs, was based on processing images of the bottom cross-section of the vessel. These were collected by a high-speed camera FASTCAM SA3 with a 45° mirror located underneath the tank, and two equal light sources located on its sides allowing the proper illumination of the system. In this way, for each stirrer speed, 500 frames short videos were obtained at a frequency of 250 fps. The main steps of the method are briefly outlined below.

I. Images are circularly cropped, only the bottom of the tank is selected as area of interest (AOI).
II. The background grey scale value, $T_{hs,}$ is evaluated as the maximum grey scale value of the images without particles. Hence, the instantaneous amount of unsuspended particles – x_{set} - is calculated, as the number of pixels with grey scale value above the background value T_{hs}. Then, the average value X_{set} is obtained on 500 cropped circular images.
III. Subsequently, the instantaneous amount of moving particles (described by x_{mov}) between a pair of frames is calculated. Consecutive images at 85 Hz frequency (one for every three frames) are selected to build moving frames, i.e., absolute difference between every *k* and *k+3* image. Then, the moving particles pixels are identified as pixels with greyscale value below the threshold T_{hm} =10. Hence, the moving fraction mean value is determined over the moving frames, obtaining X_{mov}.
IV. The parameter $f_{mov/tot}$, is defined as the ratio between X_{mov} and X_{set}, allowing to describe the condition of the tank bottom at the same time in term of moving and settled particles. Finally, the parameter is normalised on the maximum value along the rpm range, and it is plotted against the impeller speed.

The *Just Suspension* mixing condition is identified as the minimum impeller speed at which the parameter $f_{mov/tot}$ reaches the convergence results, or equally the scaled parameter $f_{mov/tot}/f_{max}$ reaches the unit value.

2.3 Acoustic Emission Data collection

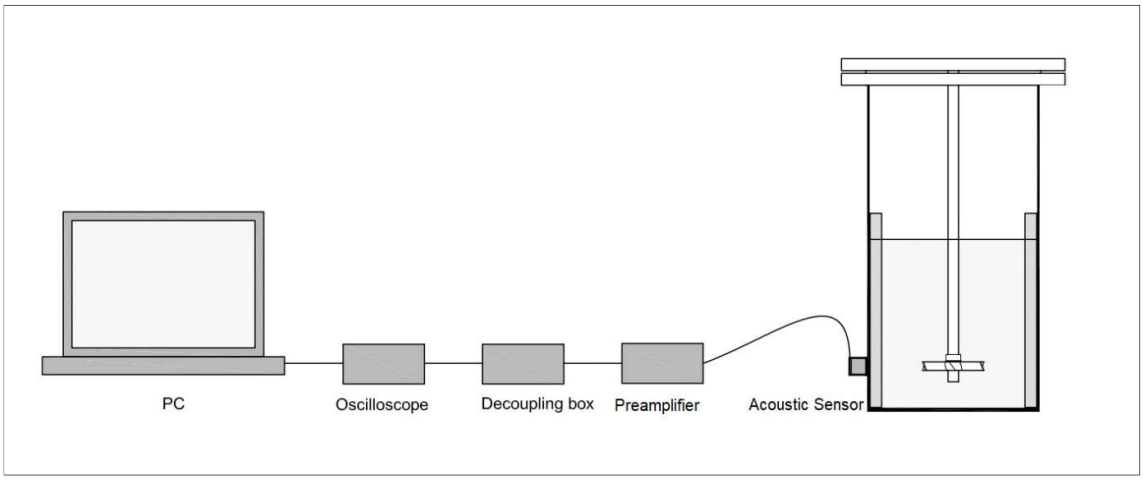

Figure 1. Schematic diagram of the experimental rig and the AE apparatus.

The acoustic equipment from Vallen Systeme (GmbH, Icking, Bavaria, Germany) was set as shown in Figure 1. A single piezoelectric acoustic sensor (VS 375M with resonance frequency of 375 kHz) was placed on the external wall of the vessel. The acoustic coupling between the surfaces was achieved by a thin layer application of water-soluble glycol (Healthlife Ultrasound Gel).
The signal was first amplified locally by using a 40 dB gain pre-amplifier (AEPH5, Vallen Systeme GmbH, Germany), connected to a conditioning (demodulating + filtering) unit (DCLP2 +28.30Vdc) where it is decoupled from the noise introduced by the amplifier.
Finally, the signal was channelled to an oscilloscope (5243b, Pico Tech Ltd, UK) and digitalised on the laptop at a sampling rate of 750 kHz - according to Shannon's Theorem (Maurice Dodson, 1992) - using Picoscope 6 software.

One hundred recordings, so-called *buffers*, each lasting 2s with a maximum amplitude of ±10 V were collected for each operating point.

2.4 Data Pre-Processing

Pre-processing steps are needed to select and organise the raw data for each classification problem, with an important focus on reducing data size.
Independent sets of experiments were carried out for glass and acrylic particles. The relative features extracted from the acoustic signal were fed to the true classification ML process. The flow chart shown in Figure 2 summarises the workflow for data processing.

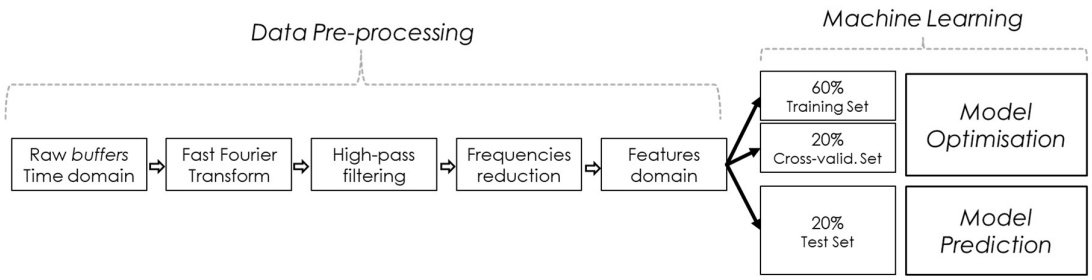

Figure 2. Workflow for data processing

Firstly, the time domain data cleaning is carried out, consisting of replacing, respectively, with ±10 and 0V, all the values that are out of range or below the detection limit of the sensor.
Voltage time signals then undergo the Discrete Fourier transformation (Cooley, Lewis and Welch, 1969) to obtain the FFT spectra and thus revealing the acoustic intrinsic fingerprint in the frequency domain. Therefore, a certain mixing condition could be identified in terms of spectrum amplitudes for specific frequency values. An illustrative example is presented in Figure 3.
A high-pass filter was applied to remove the frequencies <4 kHz, i.e. those evidently inclined to environmental interference and equipment noise (Nordon *et al.*, 2004, 2006) as confirmed from pure water recordings, from the FFT spectra.

The large data size still represents a limit for the ML data input, so a first frequency domain reduction is performed through the selection of the most significant FFT values, i.e., those with the highest relative variance.
The relative variance (RV_j) for each frequency (j-th) is defined in (2.1), where the variance σ_j^2 is weighted by the mean value μ_j following respectively the formulas (2.2) and (2.3).

$$RV_j = \frac{\sigma_j^2}{\mu_j} = \frac{\sum_{i=1}^{O} \left|a_{ij} - \mu_j\right|^2}{\sum_{i=1}^{N} a_{ij}} \tag{2.1}$$

$$\mu_j = \frac{1}{N} \cdot \sum_{i=1}^{O} a_{ij} \tag{2.2}$$

$$\sigma_j^2 = \frac{1}{O} \cdot \sum_{i=1}^{O} \left|a_{ij} - \mu_j\right|^2 \tag{2.3}$$

With:

O is the number of observations, hence the number of FFT spectra.
a_{ij} is the FFT magnitude of the *j-th* frequency (column) for the *i-th* buffer spectrum (*i-th* row).

Specifically, the frequency domain results are ordered according to decreasing RV values. The first 50,000 frequencies are selected in the primary reduction step, while the optimisation phase will further reduce the essential features.

(a)

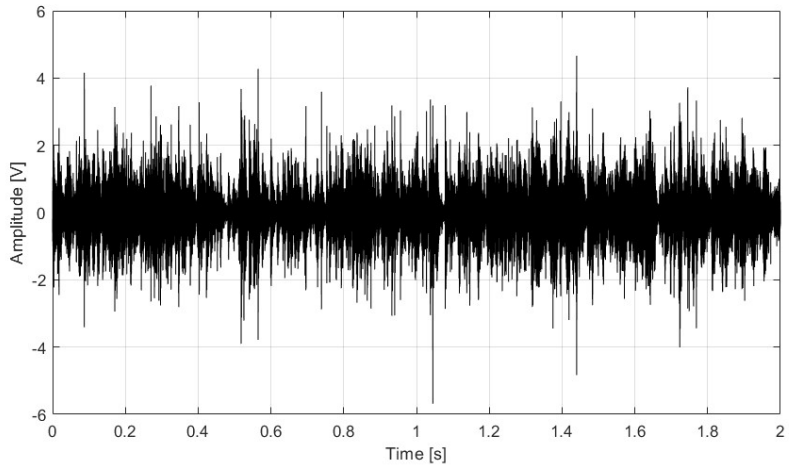

(b)

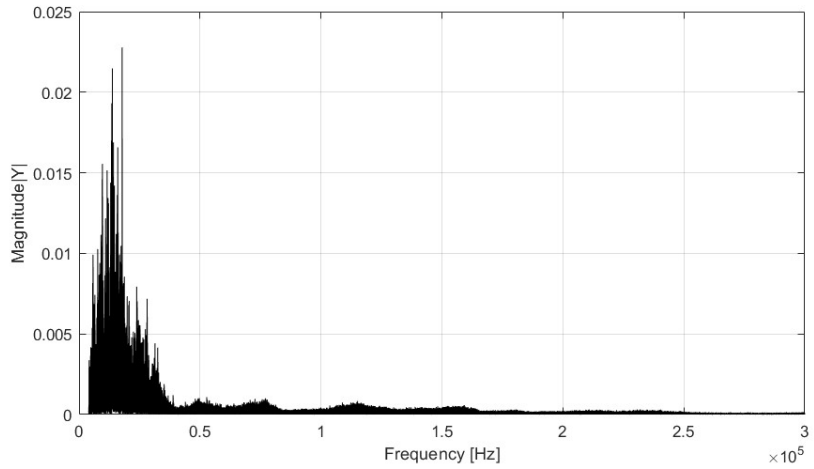

(c)

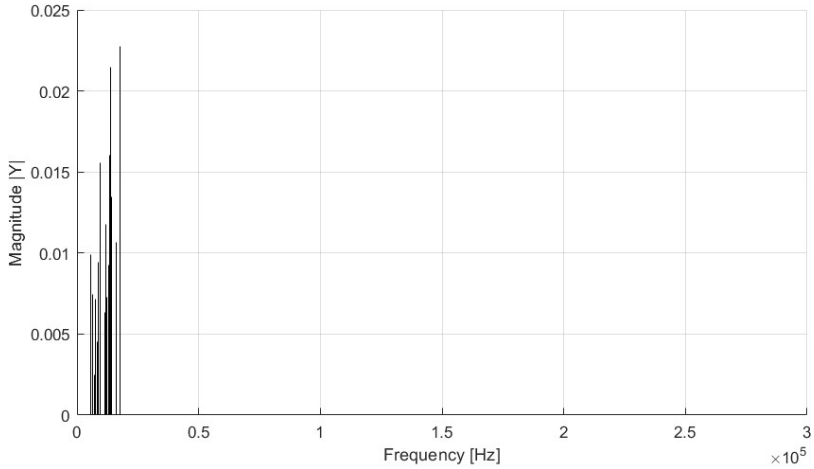

Figure 3 AE signals for dp= 4 mm N=900 rpm: (a) Time buffer, (b) FFT spectrum after high-pass filter, (c) Stem plot of the key 3,000 frequencies selected to be fed into ML task.

To make the data suitable for the Principal Component Analysis the features are scaled and mean normalised, in this way a better comparable data set is obtained where each feature distribution is mean centred and has unit variance. These steps are explained in formulas 2.4, 2.5 and 2.6.

$$F_{ij} = \frac{a_{ij} - \mu_j}{\sigma_j} \tag{2.4}$$

$$\mu_j = \frac{1}{O} \cdot \sum_{i=1}^{O} a_{ij} \tag{2.5}$$

$$\sigma_j = \sqrt{\frac{1}{O} \cdot \sum_{j=1}^{O} (a_{ij} - \mu_j)^2} \tag{2.6}$$

Finally, the global dataset, whose buffers were assigned with corresponding labels describing the belonging class (e.g., class1 partial suspension, and so on), is sub-divided into three parts i.e., the Training (60%), Cross-validation (20%) and Test dataset (20%), to guarantee that the prediction model could be built, optimised, and tested on homogeneous datasets.

2.5 Machine learning: *Optimisation and Test Phase*

The Machine Learning task is implemented in MATLAB R2019 Classification Learner Application (CLA) (MathWorks Inc, Natick, MA, USA) with the purpose to classify the provided AE data into suspension levels, basing on both input (AE) and output (the belonging classes) data. It is addressed as a classical *Supervised Classification Learning.*
In other words, once the algorithm is trained to find the hidden correspondence (or pattern) between input and output, it will be able to classify new unseen data.

To train the ML algorithm the information acquired from the alternative measurement (optical) was used as label. Such labels were used to classify the acoustic frequency spectrum that was obtained from the acquisition of the acoustic data after the pre-processing step.

A further step in the data handling was employed. The Principal component analysis (PCA) has been enabled for the CLA to further reduce data sizes and support class distinction and save computation requirement in the training and testing tasks.
The PCA is a multivariate data analysis technique (Freeman, 1992; Lastovicka and Jackson, 1992) that projects the given dataset matrix X (from the original features domain) in a smaller number dimensions named principal components (PCs) containing most of the original information. Therefore, the PCA decomposition of X can be formulated as:

$$X_{(F \times O)} = L_{(F \times P)} * S_{(P \times O)} + E_{(F \times O)} \tag{2.4}$$

Where S, the *scores* matrix, represents the dataset X in term of the PCs, ready to be fed into the classifier algorithm, while L (*loadings*) and E refer to the coefficient matrix and the unmodeled part of dataset X, respectively.

The ML optimisation phase required both Training and Cross validation sets, in determining the proper combination of number of features (frequencies) and number of principal components of PCA, hence, to guarantee better model performances, measured in terms of time required for training the model and accuracy of predictions.
In this way, the number of features (frequencies) is varied by loading into the MATLAB R2019 Classification Learner Application (CLA) (MathWorks Inc, Natick, MA, USA) the specific sub-datasets, that are simply obtained by selecting the first specific number of columns from the original 50,000 features block (this is possible because frequencies have been ranked based on relative variance values). On the other hand, the number of PC was varied on MATLAB CLA, which applied PCA on the training dataset.

The classifier model was built on the reduced Training dataset for every combination, by using best classifier algorithm (preliminary selected); and the training time is collected in turn (or turn-by-turn) to measure the ML process performance. Then, each model is tested on the cross-validation dataset, and its accuracy is evaluated following the formula 2.7.

$$Classification\ Accuracy\ [\%] = \frac{Number\ of\ correct\ predictions}{Tot\ number\ of\ observations} \cdot 100 \qquad (2.7)$$

Once the best parameters were identified i.e., the one that guarantees the better prediction accuracy, under the shorter training time, they are used to train the model with all the supervised classifier algorithms under investigation (e.g., Decision Tree, k-NN, SVM), that will then be used to recognise the suspension states from Test dataset.
It must be noted that final predictions are valued on the third unseen dataset, so the generalization ability of the model could be verified. It is important that the computer could learn from data instead of simply memorizing experiences.

3 Results and discussion

3.1 Suspension State Identification

3.1.1 Optical methodology for visual identification

Illustrative examples of pictures of the suspension, extracted from the examination of short video sequences of 2 s at 250 fps for lateral and bottom views, are reported in Figure 4. Each image represents an instantaneous of the dp= 2.5 mm acrylic beads system for different impeller speeds used for suspension state identification.

It is also interesting to focus on the bottom horizontal plane, specifically on the solid particles layout. These are distributed in an external circular region and a central cluster up to 100 rpm, while increasing the impeller speed further, vortices start moving, stretching, and dispersing the central cluster, and lifting solid particles. The JS condition has been recognised as the impeller speed at which the central zone is broken by the vortices faster than it tends to recover, applying the *Zwietering Criterion* (Zwietering, 1958) *(*i.e. no particles settled per more than 1-2s).

Results of the visual identification, including all solid-liquid systems under investigation are presented in Table 1.
The experimental data show a clear dependence of the *just suspended* condition on the particle diameter and density, as to be expected according to literature. The greater the diameter and the density, the higher is the critical speed for suspending the solid bed. Additionally, it can be observed that glass particles, despite being significantly smaller in diameter, due to the higher density have a higher N_{js} than acrylic particles.
Unlike the system with glass particles, the results obtained with the acrylic one show a weak dependency of N_{js} on particle size, in fact the solid beds are suspended at the same impeller speed (about 200 rpm).
However, it must be noted that plastic particles are characterised by a low density value (ρ=1.031 g/cm^3) that is close to the density of water. Furthermore, the subjective nature of the visual technique makes it hard to exactly discern the JS condition in case of low solid loading with low particle density values.

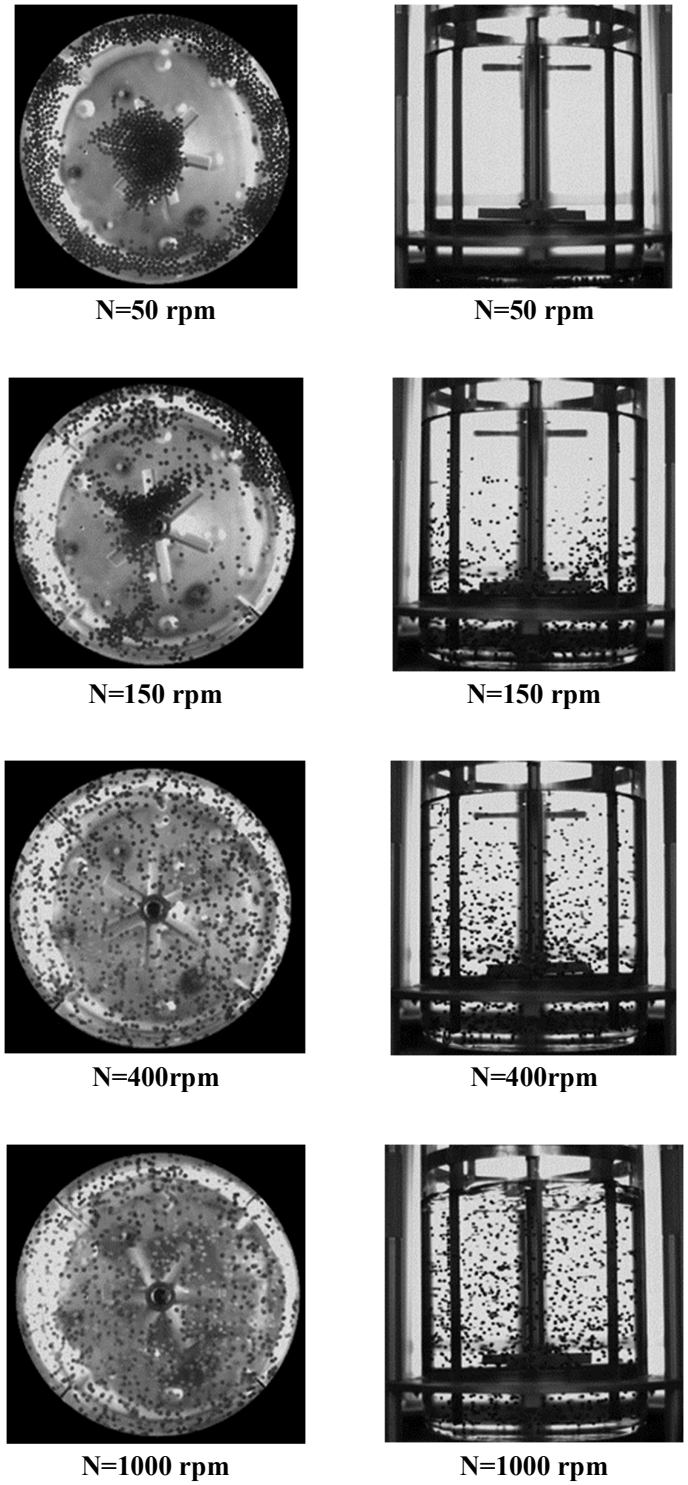

(a) Solid bed totally settled on the bottom of the Vessel

(b) Partial Suspension -On bottom suspension

(c) Complete Suspension -Off bottom suspension

(d) Uniform Suspension

Figure 4 Example of lateral and bottom pictures for Regime detection using dp=2.5mm acrylic beads, and identified suspension states:
(a) Settled bed; *(b)Partial suspension; (c) Complete suspension; (d) Uniform Suspension*

3.1.2 Optical method for image processing

The image processing technique has been applied to glass particle cases with the purpose to clearly recognise a complete dispersion condition (or JS condition*),* that has been identified as the minimum impeller speed at which the defined parameter $f_{\frac{mov}{tot}}$ reaches the convergence value, or equally the normalised parameter $f_{\frac{mov}{tot}}/f_{max}$ reaches value 1.

An illustrative example of medium size glass particle (dp= 0.650 mm) is here reported including all relative plots and quantitative results. Figure 5.a shows the normalised parameter versus the impeller speed.

The result presented complies with *Ye et al.*(Ye, Nienow and Alberini, 2019) in relation to the *f* parameter curve. It initially changes sharply with *N*, then the rpm at which it reaches the convergence value identifies the just suspended condition. The just suspended condition in this case is identified at 500 rpm.

Better understanding of the results can be obtained by focusing on the single factors from which the parameter $f_{mov/tot}$ originated from, i.e., the amount of unsuspended particles X_{set} and the amount of moving particles X_{mov}.

The trends of X_{mov} and X_{set}, whose ratio represents the $f_{mov/tot}$ parameter, are presented in Figures 5.*b* and 5.c

As expected, the unsuspended fraction X_{set} decreases with increasing impeller speeds. Particles are lifted up due to more intense vortices, being suspended and leaving the tank bottom. As a result, the number of settled particle pixels decreases.

On the other hand, the factor X_{mov} counts moving particles and presents a non-monotonic trend as a function of the impeller rotational speed. For low speeds, it shows an increasing trend because more particles begin moving on the bottom of the tank. Once the bed is suspended, X_{mov} decreases with increasing the speed because there are fewer particles moving on the bottom of the tank.

The method only detects moving (or settled) particles close to the bottom. Once the particles are suspended, they become too dark to be visualised.

(a)

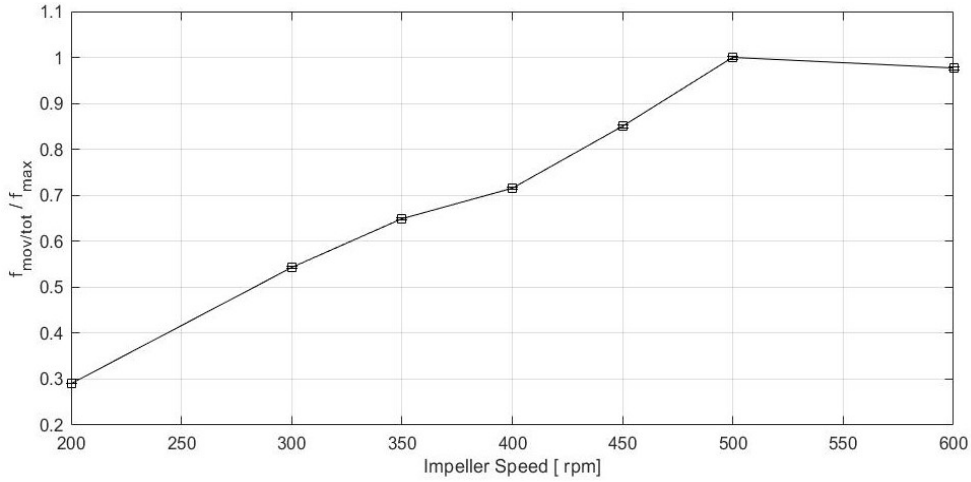

(b)

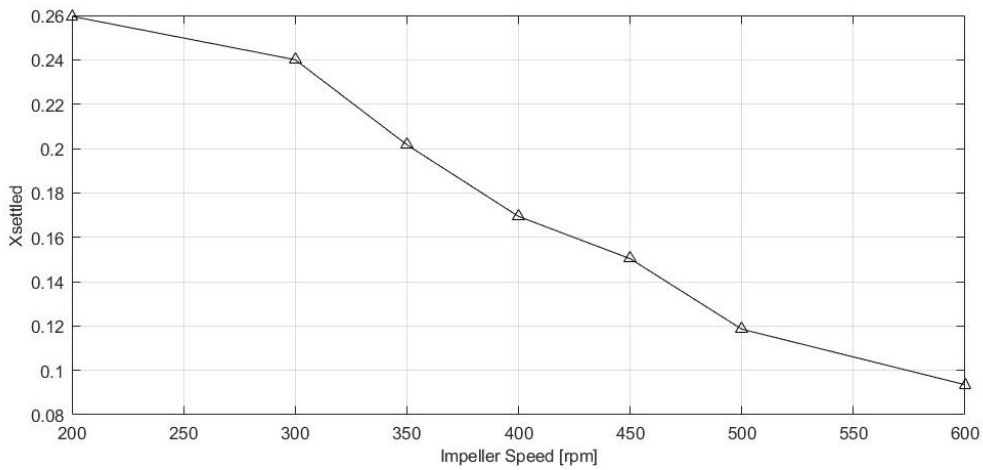

(c)

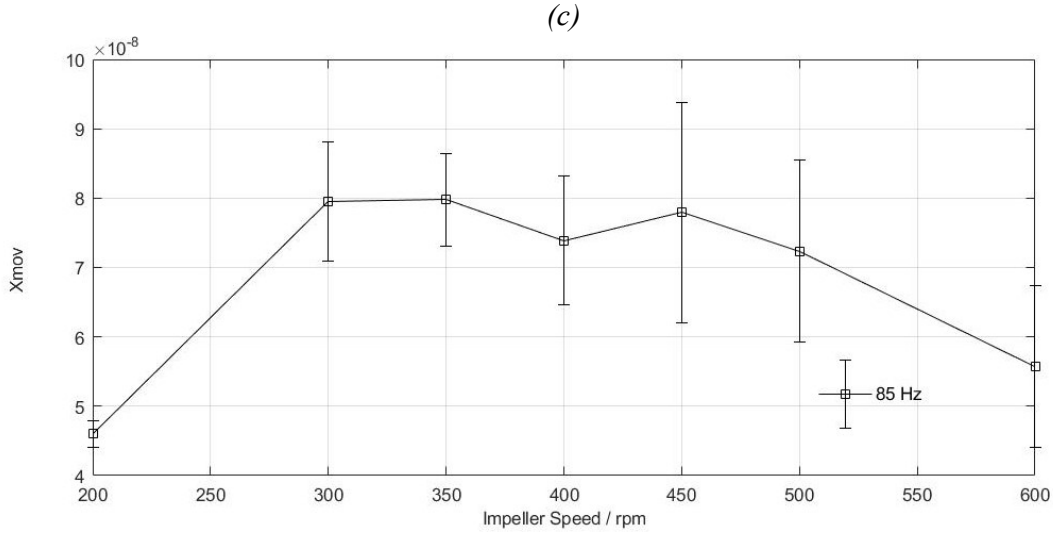

Figure 5 Example of Image processing technique for dp= 0.650 mm system:

(a) f(mov/tot)/fmax parameter for dp 0.650 mm system, using Ths=70, Thm=30,f=85Hz.

(b) X_{set} Fraction of Settled particles versus impeller speed N, using Th_s=70

(c) X_{mov} Fraction of Moving particles versus impeller speed N, using Th_m=30, f=85 Hz

The obtained JS speed is Njs=500 rpm

Table.1 presents a resuming comparison of all complementary techniques for the determination of the *just suspended* speed N_{js}.

Table.1 – (a) JS condition identification, technique comparison, (b) Nu identification

		Acrylic particles			***Glass particles***		
1(a)	d_p *[mm]*	*2.5*	*4*	*6*	*0.25*	*0.65*	*1.25*
	Njs [rpm] -*Visual Identification*	175-200	200	200	375-400	475-500	575-600
	N_{js} [rpm] - *Image processing*	-	-	-	400	500	600
1(b)	d_p *[mm]*	*2.5*	*4*	*6*	*0.25*	*0.65*	*1.25*
	*N*u [rpm] -*Visual Identification*	700	750	800	600	900	-

In general, the comparison of different methods delivers fairly consistent results. All techniques have a similar *JS* condition for all particle size cases. The obtained values appear similar, and differences are within about 50 rpm, despite the different methods and definitions of Njs.

Additionally, as shown in Table1, the comparison is extended to the Njs predicted by the Zwietering correlation(Zwietering, 1958) (with S=5.7). With the latter, the acrylic particles Njs is accurately predicted, while somewhat higher Njs are predicted for the glass beads compared to the experimental observed values. Potential disagreements with the Zwietering correlation could be due to the different mixing volumes. For instance, even though the vessel used in this study has a standard configuration, its capacity (3.25L) is lower than (from 5.5 L to 170 L) those commonly used in existing studies aimed at developing Njs.
Additionally, the Zwietering correlation has been criticised by researchers (Brucato and Brucato, 1998; Guha, Ramachandran and Dudukovic, 2007) to be conservative (i.e. to overestimate the Njs respect to their outcomes). Furthermore, a significant sensitivity of the S parameter to the geometric layout was generally detected (Ayranci and Kresta, 2014).
However, it must be noted that Zwietering correlation offers the same trends that have been observed experimentally, and also the same order of magnitude, thus supports the results obtained.

Finally, the values of N_U, the impeller speed corresponding to the beginning of uniform suspension, are also reported in Table 3.1. As expected, larger N_{US} are needed with increasing particles size and density. Indeed, the larger glass particles (dp = 1.250mm) do not achieve the homogeneous suspension, since the investigated stirrer speed is limited to 1,000 rpm. For this

reason, among the glass particles only the two smaller bead sizes were selected for the further analysis.

3.2 Classification Learner

The ML problems carried out separately on acrylic beads (2.5, 4, 6 mm particle sizes) and glass ones (0.250, 0.650 mm), have investigated the occurrence of the three suspension states, each one represented by multiple cases, i.e., three different impeller velocities for each specific particle size. In this way, the resulting global dataset totals 2,700 buffers or observations for the plastic beads and 1,800 buffers for the glass. It should be noted that the data selection and labelling follow from the previous findings presented in Section 3.1.
Once the pre-processing task, consisting of selecting the essential 50,000 frequencies (features), has been completed and the global dataset is split into three sub-ones (train, cross validation and test), the model building and optimisation steps can be carried out.

The ML optimisation phase is conducted with the optimal algorithm (preliminary tested with Matlab Classification Learner in the preliminary training step through the Holdout validation tool) within the total of 6 different ones that were investigated. The best combination of parameters (i.e., the number of components of PCA to be considered and the number of frequencies to be fed into the ML) was determined as a performance trade-off between the shorter training time (using the training set), and the more accurate classification output (using the cross-validation dataset), as shown in Figure 6 and Table 2.

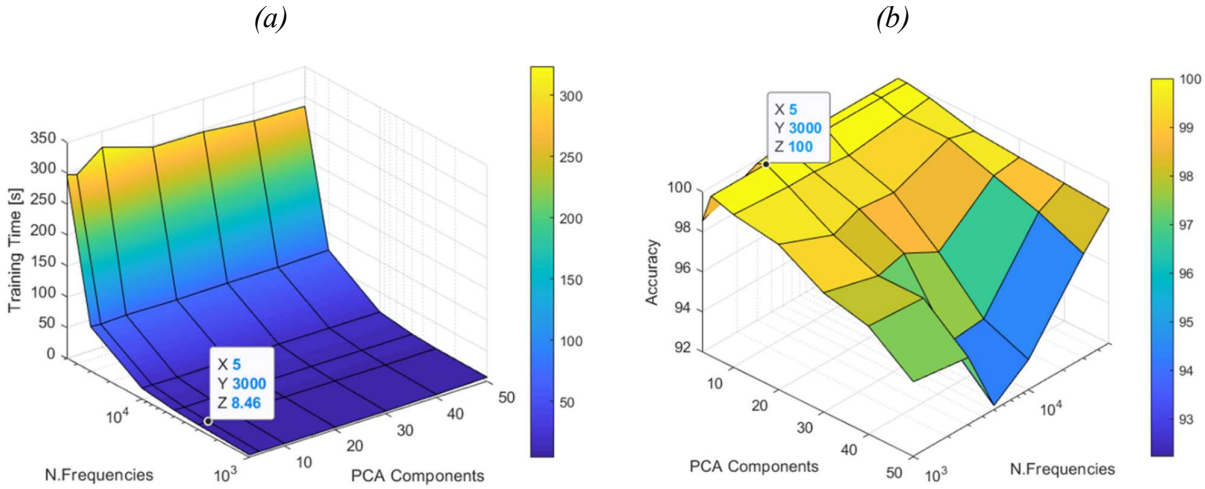

Figure 6 Example of Optimisation plots for the acrylic particles set with the SVM algorithm: Training time (a) and classification Accuracy (b) are evaluated on the parameters domain (number of frequencies vs number of PCs).

Table 2 Optimisation phase results.

System	*Optimisation Parameters*		*Model Performance Indexes*	
Acrylic	N° of Frequencies	3,000	Training Time [s]	8.5
	N° of PCs	5	Accuracy [%]	100
Glass	N° of Frequencies	30,000	Training Time [s]	60.5
	N° of PCs	3	Accuracy [%]	99.44

The tuning results seem to generally recommend manipulating a limited number of features, projected in a limited number of dimension (PCs), as highlighted in Figure 6.
Both the ML runs are optimised by using a low number of principal components (3; 5). It is a common result that most of the variance is strictly captured by the first PCs, such that a higher number of dimensions (PCs) is useless to achieve a distinction between classes. Rather, it is often redundant to tie the model to large number of PCs.
On the other hand, the number of frequencies selected is of fundamental importance, as it indicates the ease (or the complexity) relating to the specific classification. Furthermore, the optimisation graphs show that it strongly affects the model training times, which are desired to be kept as low as possible in order to develop a real-time technology.
In this perspective, it has always been possible to classify acoustic data based on a considerably reduced number of frequencies of the FFT spectrum, where the total number is reduced of several order of magnitude.
The highest classification complexity is presented for glass particles. Here, a greater number of frequencies is required to capture enough differences between the classes. Otherwise as a result of the PCA, the PCs would not have contained a sufficient variance to allow for a correct prediction.

The final test phase is completed by using the determined optimal model parameters. The machine algorithm's predicting ability is verified on the test-dataset (unseen by the machine algorithm on the previous phase) for every classification algorithm. The global results are reported in Table 3.

Table 3. Testing phase overall results: (a) *acrylic particles, (b) Glass Particles.*

3 (a)	*Classification Accuracy [%]*					
State of Suspension	Lin. SVM	Quad SVM	Cubic SVM	W. k-NN	C. k-NN	Fine Tree
Partial	100	100	100	100	100	100
Complete	100	100	99.44	100	100	99.44
Uniform	100	100	100	100	99.44	100
Tot	100	100*	99.81	100	99.81	99.81

3 (b)	*Classification Accuracy [%]*					
State of Suspension	Lin. SVM	Quad SVM	Cubic SVM	W. k-NN	C. k-NN	Fine Tree
Partial	*96.67*	*99.17*	*100*	*100*	*100*	*100*
Complete	*80*	*95*	*47.5*	*99.17*	*98.33*	*97.5*
Uniform	*50*	*79.17*	*70*	*100*	*100*	*100*
Tot	*75.67*	*91.11*	*72.50*	*99.72**	*99.44*	*99.17*

(*) The algorithm has been used for the optimisation step.

The test with acrylic particles provides fine forecasting accuracies, the precisions are greater than 99.81% for the entire range of algorithms.
The Quadratic SVM algorithm, such as linear SVM and weighted k-NN, leads to the exact prediction response (100%), while the less reliable algorithms confuse only one output, on a total of 540 test-dataset observations. The few incorrect predictions involve complete and uniform suspension classes that are confused with adjacent classes. There is no repeated misclassification.

A further confirmation of what has been already found arises from observing the dataset translation into the PCs domain. Figure7 highlights how crucial the PCA decomposition is in supporting the classification task. Indeed, the observations from the same class appear clearly divided in class clusters (red, blue, green), and sub-clustering of data at specific rpm are weakly observable. No significant overlap of classes is observed, which supports the excellent prediction outputs above.

On the other hand, the experiments for the glass particles achieved inhomogeneous results. The k-NN and fine Tree algorithms present optimal forecasting ability, higher than 99.17 %, with a very low number of misclassifications regarding partial and complete suspension states.
Conversely, the SVM algorithms (especially with linear and cubic kernel function) performed significantly poor in terms of accuracy. Most of the incorrect responses involved the complete and uniform suspension states.

From the PCs decomposition plot, in Figure 7, the dataset observations appear mostly ordered along the first principal component, but they constitute global class clusters without contiguity, i.e., formed by non-contiguous subgroups in term of particle size.
In this way, two main issues are highlighted. Firstly, an overlap between the two particles diameters is noticed dp1 (0.250mm) complete suspension and dp2 (0.650mm) partial suspension), such to lead misclassifications, as weakly noticed also for Tree and k-NN algorithms.
Secondly, the non- contiguity between class sub-cluster from different dp is probably the reason why the SVM classification algorithms performed poorly. Indeed, these models commit most of forecasting errors on complete and uniform suspension classes belonging to different particle sizes, while k-NN and fine Tree seem to not suffer this condition.

(a)

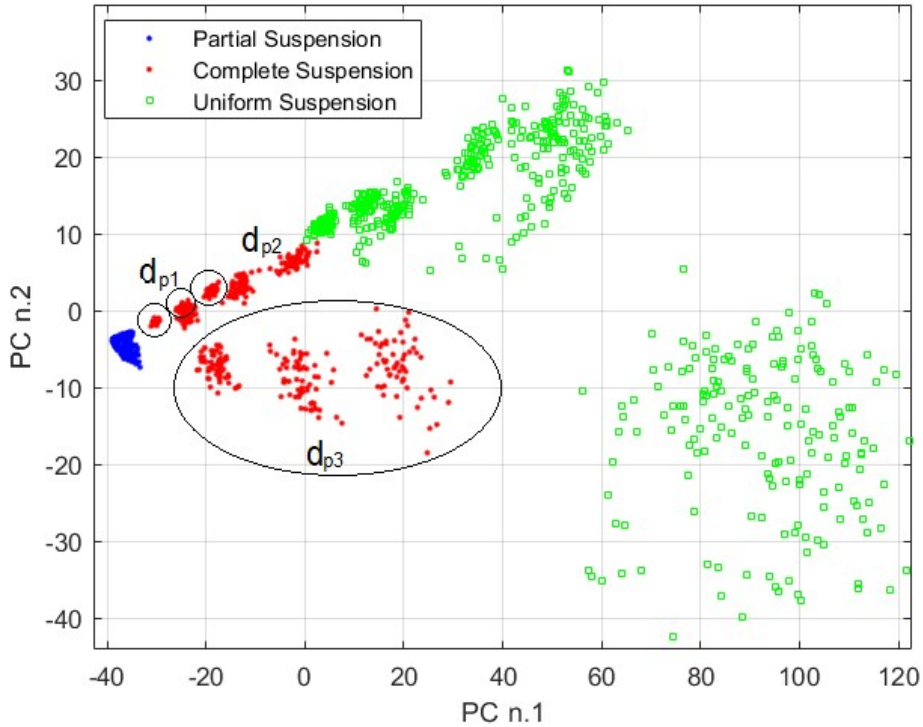

(b)

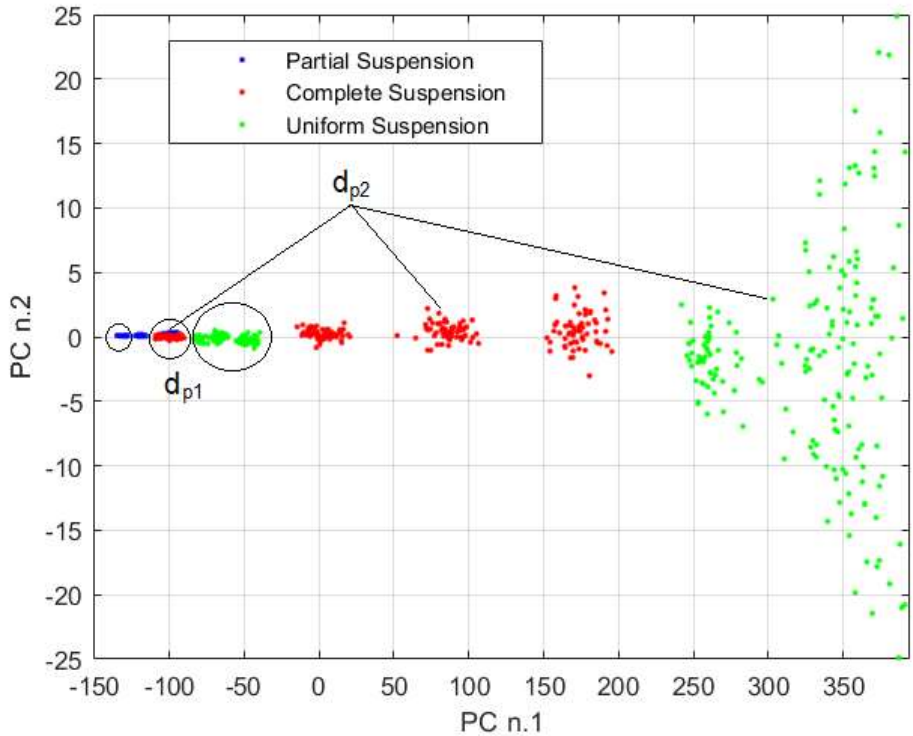

Figure 7 The dataset observations visualised in the first two PCs score domain for acrylic particles(a), and for glass particles (*b*).

4 Conclusions

In this work the AE sensing was coupled with ML to identify the suspension states for glass and acrylic beads of different sizes in a solid-liquid stirred tank equipped with a PBT-6 impeller. A single passive acoustic emission sensor has been placed directly in contact with the outer vessel wall, and the AE data was captured under different solid particle loadings along with a range of impeller velocity, leading to different mixing conditions.

Preliminary analysis of the AE has highlighted the capability to obtain clear differences in terms of the acoustic fingerprint from FFT spectrum (the higher particles inertia generated higher and more defined peaks), hence selected to be fed into the ML classification process.
Therefore, the machine was trained to recognize the partial, complete, and uniform suspensions using the essential and reduced frequencies based on higher variance. This to produce a more streamlined method with better classification performances.
To train the algorithm, alternative measurements were used such as optical methodologies which have been used extensively in previous work to characterise suspension regimes.
In particular three regimes have been characterised and as a consequence used as classification labels: partially suspended, suspended and fully suspended regimes.
The final test on the unseen dataset, concluded the ML task. The best algorithms have attained excellent predictive results: with an accuracy equal to 99.72% for glass particles, while the acrylic runs has been completed with excellent classification responses, due to excellent PCA decompositions. In fact, for acrylic particles the prediction is almost 100% despite the type of algorithm used, which suggest that the raw signal was clearly different for the three classification states. This might be related to the low concentration of particles and to a reduced interaction between the particles themselves. This might be the reason why when glass particles are employed the prediction seems more challenging and some algorithms are penalised by scoring low prediction values (circa 50%).
In fact, inhomogeneous ML results have characterized the glass particles runs among the different algorithm tested. This outcome is symptomatic of a higher complexity of this identification task due to a poor classification of the PC decomposition, also evidenced by the high number of frequencies requested to capture enough differences between the classes.

In conclusion, the combination of AE and ML has shown to allow obtaining promising results in predicting the solid suspension state and type of solids with the benefits of in situ applicability, good sensitivity, and rapid response times. Therefore, it might be further investigated to be applied as smart and complete monitoring technology, potentially capable of handling applications in real time.
This project has proposed a first comparative acoustic analysis, however more in-depth studies on AE generation and transmission within stirred tanks are worth exploring. The entire ML process would benefit in terms of improving speed and robustness.

References

Angst, R. and Kraume, M. (2006) 'Experimental investigations of stirred solid/liquid systems in three different scales: Particle distribution and power consumption', *Chemical Engineering Science*, 61(9), pp. 2864–2870. doi: 10.1016/j.ces.2005.11.046.

Ayazi Shamlou, P. and Koutsakos, E. (1989) 'Solids suspension and distribution in liquids under turbulent agitation', *Chemical Engineering Science*, 44(3), pp. 529–542. doi: 10.1016/0009-2509(89)85030-4.

Ayranci, I. and Kresta, S. (2014) 'Critical analysis of Zwietering correlation for solids suspension in stirred tanks', *Chemical Engineering Research and Design*, 92, pp. 413–422. doi: 10.1016/j.cherd.2013.09.005.

Baldi, G., Conti, R. and Alaria, E. (1978) 'Complete suspension of particles in mechanically agitated vessels', *Chemical Engineering Science*. doi: 10.1016/0009-2509(78)85063-5.

Barresi, A. and Baldi, G. (1987) 'Solid dispersion in an agitated vessel', *Chemical Engineering Science*. doi: 10.1016/0009-2509(87)87060-4.

Belchamber, R. M. *et al.* (1986) 'Quantitative Study of Acoustic Emission from a Model Chemical Process', *Analytical Chemistry*. doi: 10.1021/ac00121a058.

Bouchard, J. G., Payne, P. A. and Szyszko, S. (1994) 'Non-invasive measurement of process states using acoustic emission techniques coupled with advanced signal processing', *Chemical Engineering Research and Design*.

Bourne, J. R. and Sharma, R. N. (1974) 'Homogeneous particle suspension in propeller-agitated flat bottomed tanks', *The Chemical Engineering Journal*. doi: 10.1016/0300-9467(74)85030-6.

Boyd, J. W. R. and Varley, J. (2001) *The uses of passive measurement of acoustic emissions from chemical engineering processes*, *Chemical Engineering Science*.

Brucato, A. and Brucato, V. (1998) 'Unsuspended mass of solid particles in stirred tanks', *Canadian Journal of Chemical Engineering*, 76(3), pp. 420–427. doi: 10.1002/cjce.5450760311.

Brunazzi, E. *et al.* (2002) 'Measuring volumetric phase fractions in a gas-solid-liquid stirred tank reactor using an impedance probe', *Canadian Journal of Chemical Engineering*. doi: 10.1002/cjce.5450800407.

Brunazzi, E. *et al.* (2004) 'An impedance probe for the measurements of flow characteristics and mixing properties in stirred slurry reactors', *Chemical Engineering Research and Design*. doi: 10.1205/cerd.82.9.1250.44165.

Buurman, C., Resoort, G. and Plaschkes, A. (1986) 'Scaling-up rules for solids suspension in stirred vessels', *Chemical Engineering Science*. doi: 10.1016/0009-2509(86)80017-3.

Chowdhury, N. H. *et al.* (1995) 'An experimental investigation of solids suspension at high solids loadings in mechanically agitated vessels', in *AIChE Symposium Series*. American Institute of Chemical Engineers, p. 131.

Chowdhury, N. H. (1998) 'Improved predictive methods for solids suspension in agitated vessels at high solids loadings.'

Cleaver, J. W. and Yates, B. (1973) 'Mechanism of detachment of colloidal particles from a flat substrate in a turbulent flow', *Journal of Colloid And Interface Science*. doi: 10.1016/0021-9797(73)90323-8.

Cooley, J. W., Lewis, P. A. W. and Welch, P. D. (1969) 'The Fast Fourier Transform and its Applications', *IEEE Transactions on Education*. doi: 10.1109/TE.1969.4320436.

D. Havelkova (1987) 'Dissertation', in *CVUT FSI*. Praha.

Davis, J. *et al.* (2012) 'Smart manufacturing, manufacturing intelligence and demand-dynamic performance', *Computers & Chemical Engineering*, 47, pp. 145–156. doi: https://doi.org/10.1016/j.compchemeng.2012.06.037.

Forte, G. *et al.* (2019) 'Measuring gas hold-up in gas–liquid/gas–solid–liquid stirred tanks with an electrical resistance tomography linear probe', *AIChE Journal*. doi: 10.1002/aic.16586.

Forte, G. *et al.* (2021) 'Use of acoustic emission in combination with machine learning: monitoring of gas–liquid mixing in stirred tanks', *Journal of Intelligent Manufacturing*. doi: 10.1007/s10845-020-01611-z.

Freeman, J. (1992) 'A User's Guide to Principal Components', *Journal of the Operational Research Society*. doi: 10.1057/jors.1992.90.

Grosse, C. U. and Ohtsu, M. (2008) *Acoustic emission testing: Basics for Research-Applications in Civil Engineering*, *Acoustic Emission Testing: Basics for Research-Applications in Civil Engineering*. Springer Berlin Heidelberg. doi: 10.1007/978-3-540-69972-9.

Guerci, D., Conti, R. and Sicardi, S. (1986) 'Proc. International Colloquium on Mechanical Agitation', in.

Guha, D., Ramachandran, P. A. and Dudukovic, M. P. (2007) 'Flow field of suspended solids in a stirred tank reactor by Lagrangian tracking', *Chemical Engineering Science*, 62(22), pp. 6143–6154. doi: 10.1016/j.ces.2007.06.033.

Harriott, P. (1962a) 'Mass transfer to particles: Part I. Suspended in agitated tanks', *AIChE Journal*. doi: 10.1002/aic.690080122.

Harriott, P. (1962b) 'Mass transfer to particles: Part II. Suspended in a pipeline', *AIChE Journal*. doi: 10.1002/aic.690080123.

He, Y. J., Wang, J. D. and Yang, Y. R. (2009) 'Resolution of structure characteristics of passive acoustic emission signals in multiphase flow system', *Journal of Physics: Conference Series*, 147. doi: 10.1088/1742-6596/147/1/012008.

Hosseini, S. *et al.* (2010) 'Study of solid-liquid mixing in agitated tanks through electrical resistance tomography', *Chemical Engineering Science*. Elsevier, 65(4), pp. 1374–1384. doi: 10.1016/j.ces.2009.10.007.

Hou, R., Hunt, A. and Williams, R. A. (1999) *Acoustic monitoring of pipeline flows: particulate slurries*, *Powder Technology*. Available at: www.elsevier.comrlocaterpowtec.

Jafari, R., Tanguy, P. A. and Chaouki, J. (2012) 'Characterization of minimum impeller speed for suspension of solids in liquid at high solid concentration, using gamma-ray densitometry', *International Journal of Chemical Engineering*, 2012. doi: 10.1155/2012/945314.

Jirout, T., Moravec, J. and Rieger, F. (2006) 'Electrochemical measurement of the impeller speed for off-bottom suspension in a dish-bottomed vessel', *Inżynieria Chemiczna i Procesowa*.

Kneule, F. (1956) 'Die Prüfung von Rührern durch Löslichkeitsbestimmung', *Chemie Ingenieur Technik*. doi: 10.1002/cite.330280316.

Kubat, M. (2017) *An Introduction to Machine Learning*, *An Introduction to Machine Learning*. doi: 10.1007/978-3-319-63913-0.

L'Heureux, A. *et al.* (2017) 'Machine Learning with Big Data: Challenges and Approaches', *IEEE Access*. IEEE, 5, pp. 7776–7797. doi: 10.1109/ACCESS.2017.2696365.

Lastovicka, J. L. and Jackson, J. E. (1992) 'A User's Guide to Principal Components', *Journal of Marketing Research*. doi: 10.2307/3172717.

Lee, J., Bagheri, B. and Kao, H. A. (2015) 'A Cyber-Physical Systems architecture for Industry 4.0-based manufacturing systems', *Manufacturing Letters*. doi: 10.1016/j.mfglet.2014.12.001.

Lele, A. (2019) 'Industry 4.0', in *Smart Innovation, Systems and Technologies*. doi: 10.1007/978-981-13-3384-2_13.

'M. Bohnet, G. Niesmak, Distribution of solids in stirred suspensions, Germ. Chem. Eng. 3 (1980) 57–65.' (no date).

Maurice Dodson (1992) 'Shannon's Sampling Theorem', in *Current Science*. Current Science Association, pp. 253–260.

Micale, G., Grisafi, F. and Brucato, A. (2002) 'Assessment of particle suspension conditions in stirred vessels by means of pressure gauge technique', *Chemical Engineering Research and Design*, 80(8), pp. 893–902. doi: 10.1205/026387602321143444.

Mitchell, T. M. (1997) *Machine Learning*, *Intelligent Systems Reference Library*. McGraw-Hill Science/Engineering/Math; doi: 10.1007/978-3-642-21004-4_10.

Nagata, S. (1975) 'Mixing. Principles and applications.' doi: 10.1021/ie50537a024.

Nienow, A. W. (1968) 'Suspension of solid particles in turbine agitated baffled vessels', *Chemical Engineering Science*. doi: 10.1016/0009-2509(68)89055-4.

Nienow, A. W. (1985) 'The suspension of solid particles.', pp. 364–390. doi: 10.1016/b978-075063760-2/50037-8.

Nienow, A. W., Edward, M. F. and Harnby, N. (1997) 'Mixing in Process Industries', *Butterworth-Heinemann*. doi: 10.1007/s13398-014-0173-7.2.

Nienow, A. W., Unahabhokha, R. and Mullin, J. W. (1969) 'The mass transfer driving force for high mass flux', *Chemical Engineering Science*. doi: 10.1016/0009-2509(69)87030-2.

Nordon, A. *et al.* (2004) 'Monitoring of a heterogeneous reaction by acoustic emission', *Analyst*. The Royal Society of Chemistry, 129(5), pp. 463–467. doi: 10.1039/B402875A.

Nordon, A. *et al.* (2006) 'Factors affecting broadband acoustic emission measurements of a heterogeneous reaction', *Analyst*. doi: 10.1039/b510922a.

Paul, E. L., Atiemo-Obeng, V. A. and Kresta, S. M. (2004) *Handbook of industrial mixing: science and practice*. John Wiley & Sons.

Raghava Rao, K. S. M. S., Rewatkar, V. B. and Joshi, J. B. (1988) 'Critical impeller speed for solid suspension in mechanically agitated contactors', *AIChE Journal*. John Wiley & Sons, Ltd, 34(8), pp. 1332–1340. doi: 10.1002/aic.690340811.

Sardeshpande, M. V. *et al.* (2009) 'Solid suspension and liquid phase mixing in solid-liquid

stirred tanks', *Industrial and Engineering Chemistry Research*, 48(21), pp. 9713–9722. doi: 10.1021/ie801858a.

Shirhatti, V. *et al.* (2007) 'Determination of minimum agitation speed for complete solid suspension using four electrode conductivity method', *AIP Conference Proceedings*, 914(1), pp. 389–396. doi: 10.1063/1.2747458.

Simon, A. *et al.* (2015) 'An Overview of Machine Learning and its Applications', *International Journal of Electrical Sciences & Engineering (IJESE)*.

Špidla, M. *et al.* (2005) 'Solid particle distribution of moderately concentrated suspensions in a pilot plant stirred vessel', *Chemical Engineering Journal*, 113(1), pp. 73–82. doi: 10.1016/j.cej.2005.08.005.

Tervasmäki, P., Tiihonen, J. and Ojamo, H. (2014) 'Comparison of solids suspension criteria based on electrical impedance tomography and visual measurements', *Chemical Engineering Science*. Elsevier, 116, pp. 128–135. doi: 10.1016/j.ces.2014.05.003.

Tily, P. J. *et al.* (1988) 'Monitoring of mixing processes using acoustic emission.', *FLUID MIXING III. SYMP., BRADFORD, U.K., SEP. 8-10, 1987 (SYMP. SERIES*.

Wuest, T. *et al.* (2016) 'Machine learning in manufacturing: Advantages, challenges, and applications', *Production and Manufacturing Research*. Taylor & Francis, 4(1), pp. 23–45. doi: 10.1080/21693277.2016.1192517.

Ye, G., Nienow, A. W. and Alberini, F. (2019) 'Quantitative Measurements of the Critical Impeller Speed for Solid-Liquid Suspensions', *Chemical Engineering and Technology*, 42(8), pp. 1643–1653. doi: 10.1002/ceat.201800716.

Zwietering, T. N. (1958) 'Suspending of solid particles in liquid by agitators', *Chemical Engineering Science*. doi: 10.1016/0009-2509(58)85031-9.